ELSEVIER

Ceramics International 33 (2007) 249–253

CERAMICS INTERNATIONAL

www.elsevier.com/locate/ceramint

Synthesis and characterization of $Ba_{6-3x}Sm_{8+2x}Ti_{18}O_{54}$ microwave dielectric ceramics

Dalveer Kaur [a], Sukhleen Bindra Narang [a,*], K. Singh [b]

[a] *Department of Electronics Technology, Guru Nanak Dev University, Amritsar, Punjab, India*
[b] *Department of Physics, Guru Nanak Dev University, Amritsar, Punjab, India*

Received 17 January 2005; received in revised form 15 July 2005; accepted 12 September 2005
Available online 10 January 2006

Abstract

Dielectric ceramics in the $BaO–Sm_2O_3–TiO_2$ ternary system have been synthesized and characterized. Solid solutions with the formula $Ba_{6-3x}Sm_{8+2x}Ti_{18}O_{54}$ with $x = 0.0$, 0.2–0.7 have been synthesized, which are in the vicinity of $BaO{\cdot}Sm_2O_3{\cdot}4TiO_2$ (consistent with $x = 0.5$) ternary system. X-ray powder diffraction (XRD) analysis of synthesized specimens has been done from which lattice parameters as a function of composition (x) were determined. Crystal symmetry was found out to be orthorhombic with space group of Pbam. Scanning electron microscopy (SEM) was done to observe the microstructural details of the sintered compacts. The synthesized compacts of $Ba_{6-3x}Sm_{8+2x}Ti_{18}O_{54}$ solid solutions exhibited good dielectric properties with dielectric constant (ε') in the range of 65–73 and tangent loss ($\tan\delta$) in the range of 2×10^{-2} to 9×10^{-2}, in the frequency range of 0.3–3.0 GHz, for their possible use in microwave frequency applications.

Keywords: Tungsten bronze-type structure; Lattice constant; Dielectric constant; Tangent loss

1. Introduction

Dielectric ceramics with relatively high dielectric constant (ε') to aid miniaturization and low tangent loss ($\tan\delta$) to have high quality factor (Q) for good selectivity of the microwave components are needed to satisfy very high technical demands. These materials represent a key position in the development of electronic products in the microwave frequency regime. Many ceramic dielectrics developed so far for microwave applications were composed of mixed phases consisting of TiO_2-based compounds in multi-component systems. A series of complex perovskite families of $BaTiO_3$ and $Ba_2Ti_9O_{29}$ [1], $(Ba,Sr)TiO_3$ [2], $Ba(Zn_{1/2}Nb_{2/3})O_3$ [3], $(Zr,Sn)TiO_4$ [4] have been investigated by many researchers. Ceramic solid-solutions with the ideal formulae of $Ba_{6-3x}Re_{8+2x}Ti_{18}O_{54}$, where the x value depends on the lanthanide (Re) and compositions falling in the $BaO–Re_2O_3–kTiO_2$ ternary system have received much attention due to their essential application as microwave dielectric resonators and filters [5–7]. Kolar et al. [8] investigated $BaO–Re_2O_3–kTiO_2$ system and located the compounds at 1:1:3 and 1:1:5 [9]. Takahashi et al. studied the crystals of $BaO–Re_2O_3–kTiO_2$ with 1:1:4 [10,11]. In the ternary system, the materials composition was the most important parameter in tailoring the microwave properties. The crystal structure of $BaO–Sm_2O_3–TiO_2$ compounds has been investigated by many researchers [12,13]. This has been named as tungsten bronze type structure. This structure is made up of corners sharing TiO_6^{2-} octahedra which extends and forms a network of rhombic and pentagonal channels. These solid-solutions have different valence cations with large sized divalent Ba^{2+} and trivalent rare earth Sm^{3+}. To maintain electrostatic stability, three Ba^{2+} ions should be replaced with two Sm^{3+} ions and a vacancy. Two kinds of sites occupied by large cations exist in the tungsten bronze type structure. One is similar to the A-site in the perovskite-type ABO_3 structure, which is occupied with a maximum of ten ions of Ba^{2+} and/or Sm^{3+} in the unit cell. Another is pentagonal channel cavity which is formed among the perovskitelike columns and is occupied with a maximum of 4 Ba^{2+} ions and/or vacancies in the unit cell. If these large sites are fully occupied, the formula $Ba_6Sm_8Ti_{18}O_{54}$ should be obtained and the solid solutions so formed are hence called $Ba_6Sm_8Ti_{18}O_{54}$ solid solutions,

* Corresponding author. Tel.: +91 9356002303.
E-mail address: sukhleen2@yahoo.com (S.B. Narang).

0272-8842/$32.00
doi:10.1016/j.ceramint.2005.09.026

which are consistent with $x = 0.0$ in $Ba_{6-3x}Re_{8+2x}Ti_{18}O_{54}$ formula. It is due to the replacement of Ba^{2+} and rare earth ions that the variations in properties occur. However, it should be noted that the characteristics not only depend on the cations in A sites (e.g. Ba and Re) but also the cations in B sites, i.e. the Ti proportion of the $BaO–Sm_2O_3–TiO_2$ ceramics is also the important factor to determine the characteristics of these ceramic systems [14].

The tungsten–bronze compounds have been best utilized especially for dielectric resonators [15]. The dielectric resonators (DR) are used in microwave integrated circuits (MICs) for frequency control. They are just a ceramic pellet in the form of a parallelopiped or cylindrical disc [16]. When a continuous band of microwaves is passed through a DR, it will resonate at a discrete frequency determined by the geometry and dimensions of the pellet. The dielectric element actually functions as a resonator because of the internal reflections of electromagnetic waves at the high dielectric constant material/air boundary. This results in confinement of energy within, and in the vicinity of, the dielectric material which therefore forms a resonant structure. The material used for making DRs should have high dielectric constant (>20) to aid miniaturization and a low tangent loss (<0.005) to have high Q values. All these factors strongly depend on the lattice dynamics of the materials and the ceramic processing techniques employed. The composition chosen for the study in this research work showed high values of ε' and low values of tan δ. These materials can possibly be used as dielectric resonators. DRs are used in various types of filters and oscillators and as miniature radiating elements [15] in microwave integrated circuits. Coupling to DR is easy and can replace bulky cavity resonators in many applications. DRs, which can be made to perform the same functions as waveguide filters and resonant cavities, are, in contrast very small, stable and lightweight. The popularization of advanced dielectric resonators roughly coincides with the miniaturization of many of the other associated elements of most microwave circuits.

In this research work, ceramic solid solutions of $Ba_{6-3x}Sm_{8+2x}Ti_{18}O_{54}$ formulae with $x = 0.0$, 0.2–0.7, in the close proximity to $Ba_{4.5}Sm_9Ti_{18}O_{54}$ or $BaO–Sm_2O_3–4TiO_2$ system (corresponding to $x = 0.5$), were synthesized. The structural and microstructural properties of the prepared compacts have been observed, with respect to composition, with the help of X-ray powder diffraction (XRD) and scanning electron microscopy (SEM), respectively. Dielectric properties have been investigated in the frequency range of 0.3–3.0 GHz.

2. Experimental

Starting powders were prepared by the conventional mixed-oxide route method (ceramic method). Reagent grade $BaCO_3$ (99.9%), Sm_2O_3 (99.8%) and TiO_2 (99.9%) were used as the raw materials. In the examined composition systems, x-values on the $Ba_{6-3x}Sm_{8+2x}Ti_{18}O_{54}$ formula were fixed at 0.0, 0.2 to 0.7 and are given in Table 1. The raw powders were properly weighed and ground for 12 h by a ball mill with methanol, dried and calcined for 2 h in air at 1100 °C. The calcined powder was reground and mixed with an organic binder, that is, 3 wt.% PVA (poly vinyl alcohol), passed through a mesh screen for turning out in granular powder and to provide strength and flow ability. These were then pressed into pellets of rectangular shape of 20.3 mm in length and 10 mm breadth and cylindrical shape of 12 mm in diameter and 5 mm in thickness at a pressure of 75 kN. The compacts were then sintered in air at 1300 °C for 2 h. These sintered compacts were polished with fine emery paper to make the surfaces flat, smooth and parallel for electrical measurements.

Table 1
Compositions of the starting materials

Composition (x)	Oxide powders (mol ratios)		
	BaO	Sm_2O_3	TiO_2
0.0	6.0	4.0	18.0
0.2	5.4	4.2	18.0
0.3	5.1	4.3	18.0
0.4	4.8	4.4	18.0
0.5	4.5	4.5	18.0
0.6	4.2	4.6	18.0
0.7	3.9	4.7	18.0

Powder diffraction data were taken by the step scan method on an X-ray diffractometer with Cu Kα radiation filtered by a Ni-filter in order to determine the crystalline lattice constants of prepared ceramics. Lattice parameters were calculated based on the powder diffraction patterns using diffractions from the range $20^\circ < 2\theta < 50^\circ$. Microstructure details of the sintered surfaces were studied with the help of SEM. The bulk densities of the sintered specimens were determined by the Archimedes method (liquid displacement method) using deionized water. The microwave dielectric properties were measured with a Network Analyzer of Agilent 8714ET in the frequency range of 0.3–3.0 GHz, for the same composition range, at the room temperature.

3. Results and discussion

The X-ray diffraction patterns of $Ba_{6-3x}Sm_{8+2x}Ti_{18}O_{54}$ structure with varying values of x are shown in Fig. 1. Based on these X-ray powder diffraction patterns, the lattice parameters have been calculated by least-squares refinement of diffraction data collected with angle recording diffractometer using Ni-filtered Cu Kα radiation and are given in Table 2. Variations in parameters a, b and c with respect to x are plotted in Fig. 2. It has been observed that the lattice parameters decreased almost

Table 2
Calculated lattice parameters

Lattice parameters (Å)		
a	b	c
12.5123	22.4661	3.8669
12.2171	22.3972	3.8619
12.2183	22.3863	3.8643
12.2162	22.3824	3.8611
12.2089	22.3532	3.8441
12.2042	22.3413	3.8332
12.1958	22.3246	3.8311

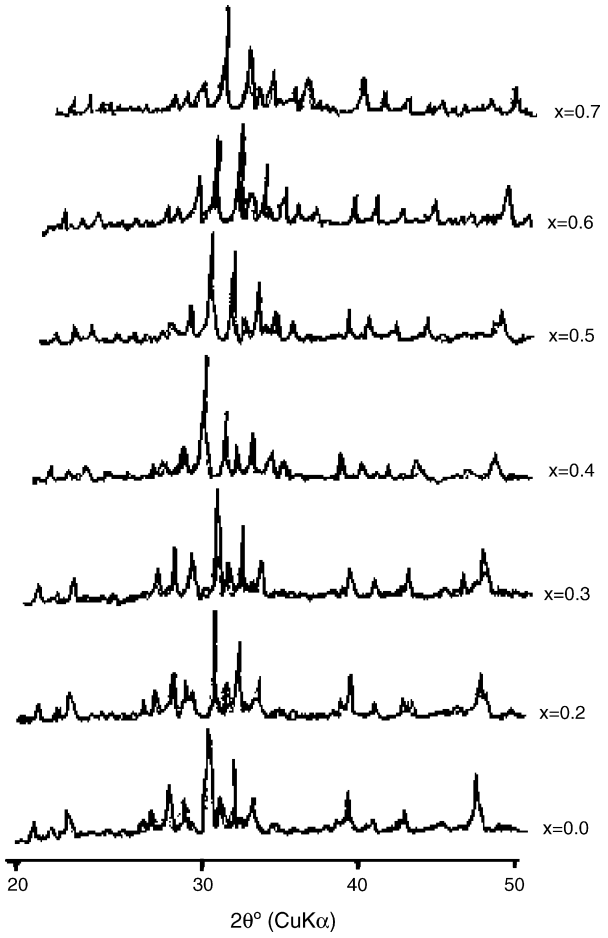

Fig. 1. X-ray diffraction patterns for $Ba_{6-3x}Sm_{8+2x}Ti_{18}O_{54}$ at sintering temperature of 1300 °C.

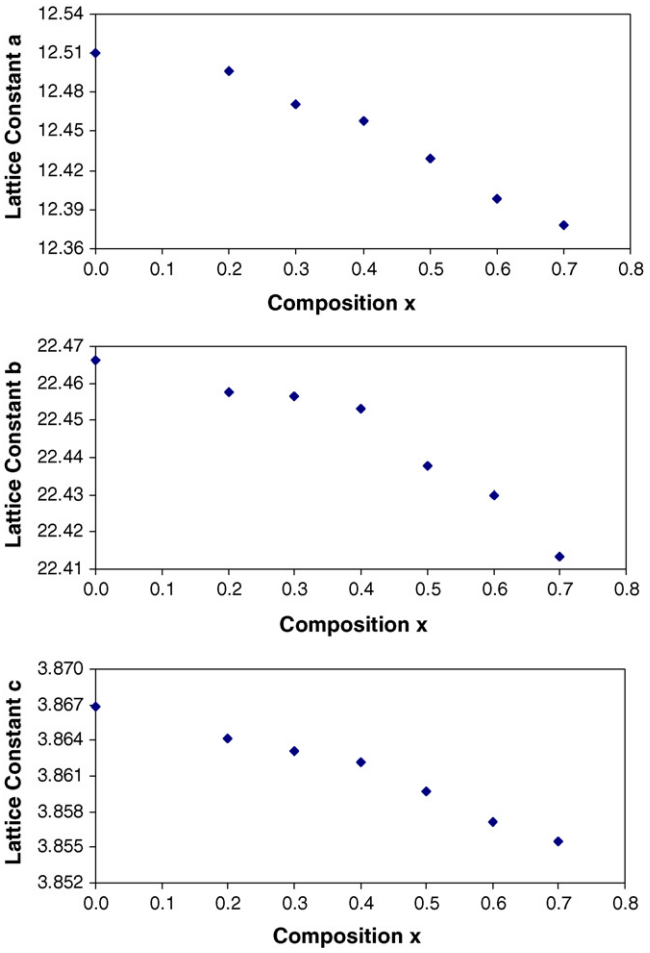

Fig. 2. Lattice parameters of $Ba_{6-3x}R_{8+2x}Ti_{18}O_{54}$ solid-solutions as a function of the composition (0.0, $0.2 \leq x \leq 0.7$).

linearly with increasing value of x. The changes in parameters satisfied the Vegard's Law [11,19]. Actually, Vegard's Law is an approximate empirical rule which holds that a linear relation exists, at constant temperature, between the crystal lattice constant of a compound and the concentration of the constituent elements. Here, parameters decreased as the amount of substitution of Sm for Ba increased, which was attributed to the change in ionic radius. XRD data confirmed that the unit-cell had orthorhombic symmetry and a possible space group was No. 55 Pbam. The lattice parameter changes were observed to be maximum for the b-axis and minimum for the c-axis. With respect to the changes per Å, the minimum change was 0.28% for a-axis with maximum of 0.39% for c-axis, but 0.36% for b-axis. This change in a, b and c dimensions was due to the ionic difference of Ba and Sm ions. It was observed that the values of lattice constants were maximum for composition $x = 0.0$, but decreased gradually as the composition increased to $x = 0.7$. This was due to the reason that as the composition increased the Sm content increased and these medium sized valence cations substituted Ba and Ti ions. Hence, the unit cell parameters decreased with this substitution. It was observed from the powder patterns of the crystallized samples that major peak occurred at 30° diffraction angle. But the peak heights lowered as the angle increased. This was because of a different type of ion substitution for Ba sites of the crystal structure.

SEM micrographs of sintered surfaces are shown in Fig. 3. It was observed in these photographs that the samples were constructed with several phases. The major phase (phase A) was light (white) phase that was observed to be the phase in the vicinity of $BaO–Sm_2O_3–4TiO_2$ of irregular shape randomly distributed. Its concentration was maximum for $x = 0.0$ and 0.6, shown in micrograph (a) and (d), respectively, but decreased for $x = 0.2$ and 0.4 shown in micrograph (b) and (c), respectively. A light grey phase (phase B) was comprised of many small and needle-like (acicular) crystals oriented at random. This phase showed the presence of the Sm content in the compound. The long acicular grains grew at the expense of short ones, especially for $x = 0.4$, which resulted in the formation of new voids where the shorter grains were originally located. The dark grey phase (phase C) formed islands of large irregular shape for $x = 0.0$ and 0.2, shown in micrographs (a) and (b) respectively, but decreased for $x = 0.4$ and 0.6. This was most likely due to shorter sintering time or improper sintering. There was another unknown dark (black) phase that existed as a small area and was observed to be dispersed in the compound can be seen in the micrographs. This phase grew into larger black areas for $x = 0.2$, 0.4 and 0.6. The values of bulk density of the sintered samples was also found out and shown in Fig. 4. The values first increased up to $x = 0.4$ but after that decreased. This was mainly

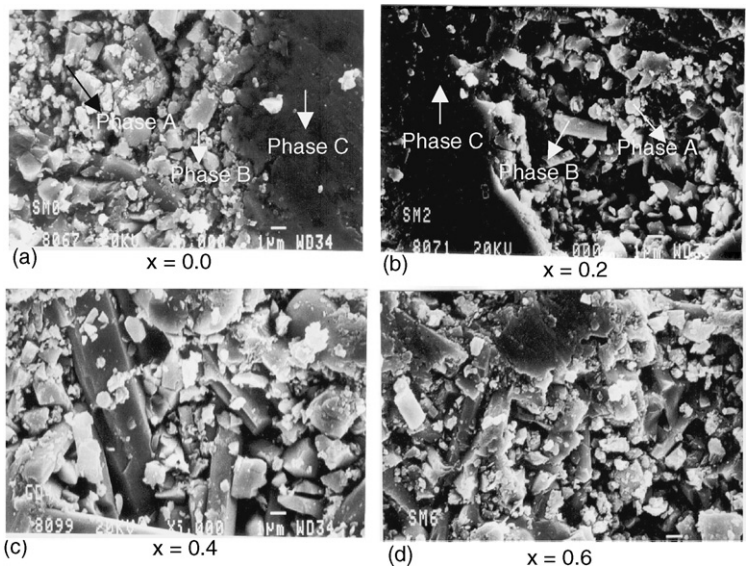

Fig. 3. SEM micrographs of compacts sintered at 1300 °C.

due to the long acicular grains came into contact and their continual growth might squeezed them away from one another, which resulted in the formation of new and larger vacant positions. This caused expansion of the space between bar-shaped grains and resulted in the increased porosity and hence decreased in the bulk densities, especially after $x = 0.4$, which can also be seen in micrographs.

The variation of ε' with frequency at room temperature for the series of synthesized ceramics is shown in the Fig. 5. It was observed that ε' decreased with frequency. Similar response has been observed by other researchers [2,15,20]. It was also observed that ε' decreased with the composition (x). The

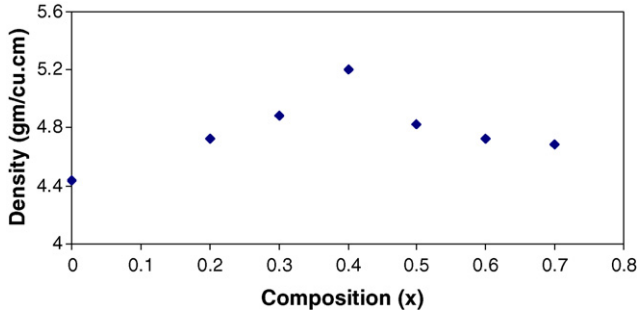

Fig. 4. Density (in gm/cm^3) as a function of composition.

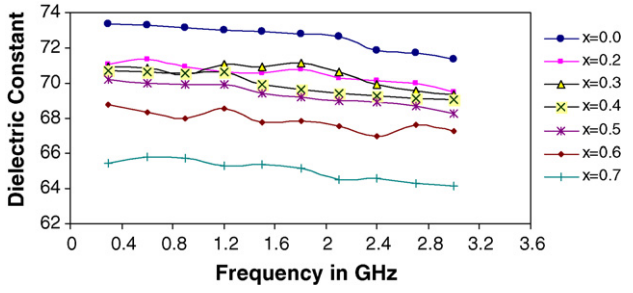

Fig. 5. Variation of dielectric constant of the compacts as a function of operating frequency (in GHz).

maximum value of ε' was observed to be 73 for $x = 0.0$ at 0.3 GHz. However, the typical performances of $\varepsilon' = 65$–73 were obtained. It was observed that ε' is maximum at $x = 0.0$, but decreased to 65 for $x = 0.7$ through 69 at $x = 0.5$. In normal behaviour, the ε' decreases with increasing frequency due to the fact that beyond a certain frequency of the applied electric field the particle exchange does not follow the alternating field [17]. The low frequency rise in dielectric constant is attributable to the interfacial effects. These take place at the contacts or in the bulk of the material at the grain boundaries. Charge is able to accumulate at these interfacial sites and thereby able to contribute to the total capacity or dielectric permittivity or dielectric constant. As the frequency is raised, eventually the system can no longer follow the time-dependent charge fluctuations and ε' tries to settle down to a value equal to the one without the interface charges. This explanation was from the frequency point of view only. But the dielectric behaviour is also dependent upon the physics of the materials. As the frequency is increased, the next polarizability is associated with the material rather than interfaces. Actually, the tungsten–bronze structure originates by diffusion of a dopant which creates distortion or defect in the perovskite structures. These perovskites have oxygen vacancies that will exhibit a dipolar polarization. However, it is possible to control the number of vacancies in the manufacturing process by proper doping. As the frequency is increased again, into the range above 2.0 GHz, there will be contribution due to the ionic separation of the components of a material. The electronic cloud associated with a unit cell is slightly distorted. So, in the octahedron associated with these kinds of materials, the unit cell has a dipole moment, which will contribute to the polarization. Eventually, the charges will no longer be able to follow the external field and the polarizability and therefore the ε' decreases to a new plateau.

The tangent loss ($\tan\delta$) was observed to be low for the prepared samples. Minimum value that was observed was 0.02 at 0.9 GHz for $x = 0.0$. It increased to 0.09 with the

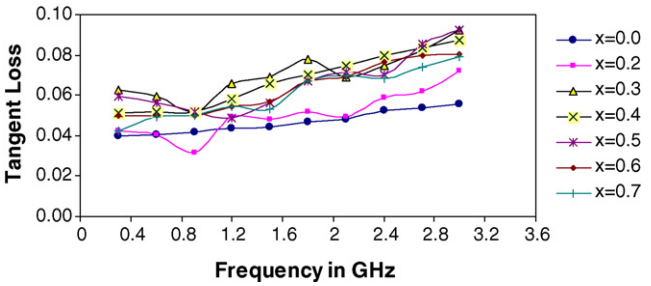

Fig. 6. Variation of tangent loss as a function of operating frequency (in GHz).

composition up to $x = 0.5$, but after that decreased to 0.049 for $x = 0.7$. This was basically due to the presence of inhomogeneties in the structure. But for $x = 0.6$ and 0.7 the rare earth concentration was more and dopants might have substituted well in sites. However, it increased with frequency and it is plotted in Fig. 6. In the dielectric materials defects, space charge formation, lattice distortions, etc in the boundaries produce an absorption current resulting in a dielectric loss (ε''). The tangent loss depends on dielectric loss (ε'') as $\tan\delta = \varepsilon''/\varepsilon'$, so it varies proportionally with ε''. In the low frequency range, ε'' is dominated by the influence of ion conductivity. The variation of ε'' in the lower microwave range is mainly caused by dipolar relaxation and absorption in the above range is mainly due to atomic and electronic polarization [18]. That is why, it increased with frequency up to 3 GHz.

4. Conclusion

In summary, complex ceramics $Ba_{6-3x}Sm_{8+2x}Ti_{18}O_{54}$ with $x = 0.0$, 0.2–0.7 were synthesized and characterized for their structural and dielectric properties. It was observed that lattice parameters decreased linearly with composition with the help of X-ray powder diffraction data. Crystals of the orthorhombic phase were obtained with the possible space group of Pbam. SEM micrographs confirmed the existence of multiphase system in the sintered compacts. The microwave dielectric properties were observed to be quite good. The typical dielectric performances of $\varepsilon' = 65$–73 were obtained. Minimum tangent loss was 2×10^{-2} for 0.0 at 0.9 GHz. However, the tangent loss increased with the composition and frequency. $Ba_{6-3x}Sm_{8+2x}Ti_{18}O_{54}$ ceramics in the vicinity of $BaO–Sm_2O_3–4TiO_2$ phase, with high dielectric constant values and low loss could be the promising materials for applications in microwave resonators.

References

[1] J. Petzelt, T. Ostapchuk, A. Pashkin, I. Rechestky, J. Eur. Ceram. Soc. 23 (14) (2003) 2627–2632.
[2] H.V. Alexandru, C. Berbecaru, A. Ioachim, M.I. Toacsen, L. Nedelcu, D. Ghetu, Mater. Sci. Eng. B 109 (2004) 152–159.
[3] S. Kamba, H. Hughes, D. Noujini, S. Surendran, R.C. Pullar, J. Petzelt, R. Freer, N.M. Alfrod, D.M. Iddles, J. Phys. D: Appl. Phys. 37 (2004) 1980–1986.
[4] H. Sreemoolanadhan, R. Ratheesh, M.T. Sebastian, J. Philip, J. Phys. D Appl. Phys. 30 (1997) 1809–1814.
[5] D. Kolar, Z. Stadler, S. Gaberscek, D. Suvorov, Ber. Dtsch. Keram. Ges. 55 (364) (1978) 346–348.
[6] D. Kolar, S. Gaberscek, H.S. Paker, B. Volavsek, J. Solid State Chem. 38 (158) (1981) 158–164.
[7] X.M. Chen, Y. Suzuki, G.L. Lu, N. Sato, J. Solid State Chem. 6 (10) (1995) 438–441.
[8] D. Kolar, S. Gaberscek, B. Volavsek, H.S. Parker, R.S. Roth, J. Solid State Chem. 38 (158) (1981) 158–164.
[9] M. Valant, D. Sovorov, D. Kolar, Jpn. J. Appl. Phys. 35 (1996) 144–150.
[10] H. Ohsato, T. Ohhashi, H. Kato, S. Nishigaki, T. Okuda, Jpn. J. Appl. Phys 32 (1995) 4312–4315.
[11] H. Ohsato, H. Kato, M. Mizuta, S. Nishigaki, T. Okuda, Jpn. J. Appl. Phys. 34 (1995) 5413–5417.
[12] W. Wersing, Solid-states Mater. Sci. 1 (5.) (1996).
[13] S.-W. Jung, J.-H. Lee, J.-J. Kim, H.-Y. Lee, S.-H. Cho, Mater. Chem. Phys. 79 (2–3) (2003).
[14] H. Ohsato, J. Eur. Ceram. Soc. 21 (15.) (2001).
[15] C.-F. Yang, Jpn. J. Appl. Phys. 39 (2000) 1430.
[16] J.S. Fiedziszko, Microwave J. (1986) 189.
[17] M. Golio, in: The RF and Microwave Handbook, CRC Press, 2001.
[18] L.F. Chen, C.K. Ong, C.P. Neo, V.V. Varadan, V.K. Varadan, in: Microwave Electronics: Measurement and Materials Characterization, John Wiley & Sons, Ltd., 2004.
[19] H. Ohsato, T. Ohhashi, S. Nishigaki, T. Okuda, K. Sumiya, S. Suzuki, Jpn. J. Appl. Phys. 32 (1993) 4323–4326.
[20] C.-L. Huang, Y.-C. Chen, Mater. Sci. Eng. A 345 (1–2) (2003) 106.